

STATIC STATE ESTIMATION OF POWER SYSTEMS CONTAINING SERIES AND SHUNT FACTS CONTROLLERS

E. A. Zamora^{1,2} and C.R. Fuerte-Esquivel¹

Faculty of Electrical Engineering¹
Universidad Michoacana de San Nicolás de Hidalgo
Morelia, Mich., México
cfuerte@zeus.umich.mx

Faculty of Engineering²
Universidad Autonoma del Carmen
Ciudad del Carmen, México

Abstract – This paper proposes a practical Flexible AC Transmission Systems (FACTS) devices implementation into a Weighted Least Squares (WLS) state estimation algorithm. FACTS devices implemented in the estimator are the Thyristor Controlled Series Compensator (TCSC), the Static Var Compensator (SVC) and the Unified Power Flow Controller (UPFC). The developed estimator upgrades the state variables of these devices simultaneously with the state variables of the rest of the electric network, for a unified solution in a single-frame of reference. Results are presented to show the developed program characteristics to assess the power system state and to set the FACTS controllers parameters for given control specifications.

Keywords: State Estimation, FACTS controllers, Weighted Least Squares

1 INTRODUCTION

Worldwide transmission systems are undergoing continuous changes stem mainly from the strong increase in interconnected power transfers, opening of the market for delivery of cheaper energy to the customers, and economic and ecological constraints which delay the building of new transmission facilities. Since the construction of new transmission lines cannot keep pace with the growing power plant capacity and energy demand, operators are looking for ways to utilise the existing power lines more efficiently, operating the grid in ways not originally envisioned. The need for more efficient power systems management, and the fast development of power electronics based on new and powerful semiconductor devices, have given raise to innovative technologies, such as Flexible AC Transmission Systems (FACTS) [1]. FACTS give utilities the benefit of deferring new line construction while increasing capacity and flexibility of existing transmission lines due to unprecedented capabilities to fully control active and reactive power flows, in magnitude and direction, to modulate voltages at specific nodes, and to fast respond to system transients.

Extensive research has been carried out in the last decade in the development of steady-state mathematical models of FACTS controllers, and their implementation in software tools used by planning and operation engineers to assess the steady-state power system performance. Among them, FACTS models and their implementation for power flow and optimal power flow

analysis have reached maturity [2]. However, despite the topic of power systems state estimation has been intensively studied since the work of Schweppe, Wildes and Rom in the late 60's [3-5], little progress has been done in the area of power system state estimation embedded with FACTS devices [6].

Power systems state estimation is the process carried out in energy control centres (ECC) in order to provide the best estimate of what is happening in the system based on real-time system measurements and a predetermined system model [7]. A redundant set of real-time measurements are collected from the entire network through the supervisory control and data acquisition (SCADA) system. Usually the measurements are branch power, nodal voltage magnitudes, or nodal power injections. These measurements are transmitted to the ECC and subjected to a statistical analysis in order to assess the system's state. Since transmitted measurements are usually corrupted by errors, this erroneous data should be filtered to eliminate bad measurements and minimise the effect of random measurement noise. This is accomplished with the help of a supplementary function called bad data processing. If after this analysis all state variables can be estimated using the available measurements, a system is said to be observable. Once an accurate estimation has been carried out, the entire system quantities such as branch power flows, line current magnitudes and nodal power injections can be calculated.

Owing to the fact that in deregulated power systems the pattern of power flows in the network is less predictable than it is in vertically integrated systems, together with the ongoing FACTS controllers installation projects, the implementation of FACTS state estimation software is crucial for the accurate real-time information about the power system operation. Bearing this in mind, this paper extends a Weighted Least-Square (WLS) state estimation algorithm to include FACTS controllers models associated to TCSC, SVC and UPFC. The program estimates FACTS controllers parameters along with the power systems state variables in a unified single-frame of reference. In this case, it is possible to estimate the FACTS controllers parameters under normal power system operation or to set these parameters in order to achieve control specifications. Test results are presented which demonstrate the effectiveness of the formulation and implementation algorithm.

2 WLS STATE ESTIMATION ALGORITHM

WLS algorithms and their variants remain the dominant techniques used in most state estimation practical programs [7]. The purpose of a static state estimator in electric power systems is to find the best estimate state \hat{x} of the true state x which best fits the measurements z through the model [3,7],

$$z = h(\hat{x}) + \varepsilon \quad (1)$$

where $z \in \mathbb{R}^m$ is the measurement vector, $\hat{x} \in \mathbb{R}^n$ is the state variable vector, $h(\cdot) \in \mathbb{R}^m$ is a nonlinear vector function relating state variables and measurements, and $\varepsilon \in \mathbb{R}^m$ is the measurement error vector with normal distribution.

State Estimation is formulated as a classical WLS estimation problem of overdetermined nonlinear equations. In this case, \hat{x} is estimated by minimising the simple unconstrained optimization problem [7],

$$J(\hat{x}) = (z - h(\hat{x}))^t R^{-1} (z - h(\hat{x})) \quad (2)$$

where $R = \text{diag}(\sigma_{ii}^2)$ is the error covariance matrix. The optimality condition to minimise $J(\hat{x})$ is given by,

$$\partial J(\hat{x}) / \partial x = H(\hat{x})^t R^{-1} (z - h(\hat{x})) = 0 \quad (3)$$

where $H(\hat{x}) = \partial h(\hat{x}) / \partial x$ is the Jacobian matrix of the measurement functions. To solve (3), only the first order approximation of $\partial J(\hat{x}) / \partial x$ expanded in a Taylor's series is considered. The resulting equation is [7],

$$G(\hat{x}^k) \Delta \hat{x}^k = (H(\hat{x}^k))^t R^{-1} (z - h(\hat{x}^k)) \quad (4)$$

where $G(\hat{x}^k) = (H(\hat{x}^k))^t R^{-1} H(\hat{x}^k)$ is the gain matrix. Equation (4) is solved iteratively for $\Delta \hat{x}^k$ and the new corrected state vector is given by $\hat{x}^{k+1} = \hat{x}^k + \Delta \hat{x}^k$. The optimal state vector \hat{x} is found if suitable convergence criteria, e.g. $|\Delta \hat{x}^k| < TOL$, is fulfilled.

3 FACTS DEVICES MODELLING FOR STATE ESTIMATION

The steady-state FACTS controller models suitable for their implementation of the classical WLS state estimation algorithm are presented in this section.

3.1 Thyristor Controlled Series Capacitor

Figure 1 shows the general configuration of a TCSC module with a fundamental frequency TCSC equivalent reactance, as function of the TCSC firing angle, α_{TCSC} , given by (5) [2],

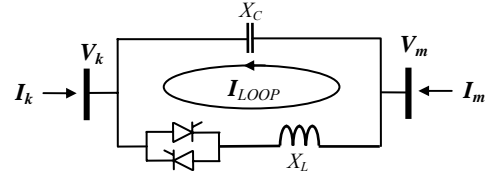


Figure 1: TCSC module

$$X_{TCSC(i)} = -X_C + (X_C + X_{LC}) \left(\frac{2(\pi - \alpha) + \sin(2(\pi - \alpha_{TCSC}))}{\pi} \right) - \frac{4X_{LC}^2 \cos^2(\pi - \alpha_{TCSC}) \left(\frac{k \tan(k(\pi - \alpha_{TCSC})) - \tan(\pi - \alpha_{TCSC})}{\pi} \right)}{X_L} \quad (5)$$

The term X_{LC} corresponds to the parallel combination of the TCSC inductive and capacitive fixed reactances, $k = \omega_0 / \omega$, where ω is the frequency of the system, and $\omega_0 = 1/\sqrt{LC}$.

The active power flow flowing through the controller from its terminal k is given by,

$$P_k^{TCSC} = \frac{V_k V_m \sin(\theta_k - \theta_m)}{X_{TCSC(i)}} \quad (6)$$

At the k^{th} iteration, the incremental change of the estimated TCSC's firing angle is $\Delta \alpha_{TCSC}^k = \alpha_{TCSC}^{k+1} - \alpha_{TCSC}^k$.

3.2 Static VARs Compensator

The SVC model including the explicit representation of the step-down transformer is shown in Figure 2 [2]. Both components are combined to form a single model, which allows direct voltage magnitude control at the high-voltage side of the transformer. In this case, the firing angle α_{SVC} is adjusted, within limits, to constraint a voltage magnitude V_k at a specified value.

The total admittance of the combined SVC-transformer set, \bar{Y}_{T-SVC} , as seen from the high-voltage side of the transformer, consists of the series combination of admittances \bar{Y}_T and \bar{Y}_{SVC} ,

$$\bar{Y}_{T-SVC} = G_{T-SVC} + jB_{T-SVC} \quad (7)$$

where

$$G_{T-SVC} = \frac{R_T}{R_T^2 + X_{Eq}^2} \quad B_{T-SVC} = -\frac{X_{Eq}}{R_T^2 + X_{Eq}^2} \quad (8)$$

$$X_{Eq} = X_T + X_{SVC} \quad X_{SVC} = \frac{X_C X_{TCR}}{X_C - X_{TCR}} \quad (9)$$

$$X_{TCR} = \frac{\pi X_L}{2(\pi - \alpha_{SVC}) + \sin(2\alpha_{SVC})} \quad (10)$$

The active and reactive power flow equations injected at node k by the single model are,

$$P_k^{T-SVC} = V_k^2 G_{T-SVC} \quad Q_k^{T-SVC} = -V_k^2 B_{T-SVC} \quad (11)$$

At the k^{th} iteration, the SVC's firing angle is upgraded by $\alpha_{SVC}^{k+1} = \alpha_{SVC}^k + \Delta \alpha_{SVC}^k$. A simplified model can be obtained considering a lossless SVC-transformer representation by an adjustable shunt susceptance B_{T-SVC} [2].

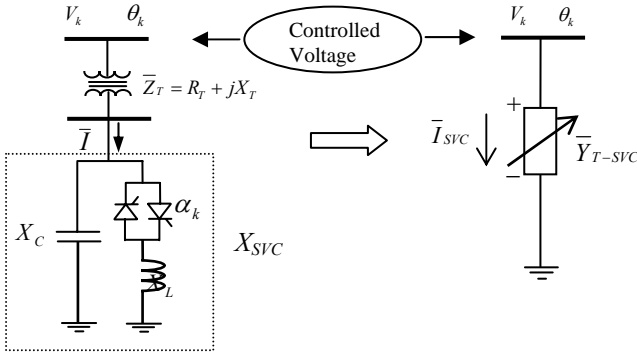


Figure 2: Combined SVC-transformer representation.

3.3 Unified Power Flow Controller

The basic principles of the UPFC operation have been already established in the open literature [8]. It follows from that discussion that an equivalent circuit consisting of two coordinated synchronous voltage sources should represent the UPFC adequately for the purpose of fundamental frequency steady-state analysis. Such an equivalent circuit is shown in Figure 3 [2].

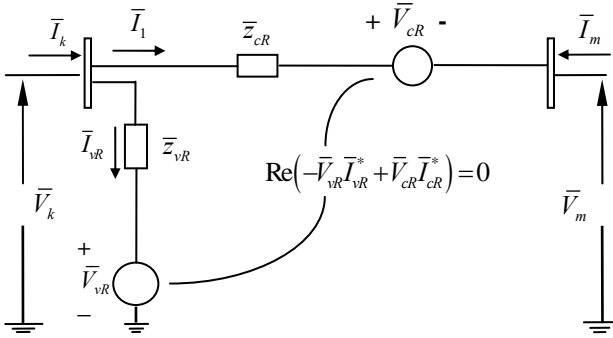


Figure 3: UPFC equivalent circuit.

The synchronous voltage sources \bar{V}_{cR} and \bar{V}_{vR} represent the fundamental Fourier series component of the switched voltage waveforms at the AC converter terminals of the UPFC. The impedances \bar{Z}_{cR} and \bar{Z}_{vR} represent coupling transformers. The UPFC general power flow equations at both terminals are as follows [2]:

The active and reactive powers flowing through the controller from its terminal k to terminal m are given by (12) and (13), respectively. Equations representing active and reactive power flowing from nodes m to k are given by (14) and (15), respectively.

$$P_{km} = V_k^2 G_{kk} + V_k V_m (G_{km} \cos(\theta_k - \theta_m) + B_{km} \sin(\theta_k - \theta_m)) + V_k V_{cR} (G_{km} \cos(\theta_k - \theta_{cR}) + B_{km} \sin(\theta_k - \theta_{cR})) + V_k V_{vR} (G_{vR} \cos(\theta_k - \theta_{vR}) + B_{vR} \sin(\theta_k - \theta_{vR})) \quad (12)$$

$$Q_{km} = -V_k^2 B_{kk} + V_k V_m (G_{km} \sin(\theta_k - \theta_m) - B_{km} \cos(\theta_k - \theta_m)) + V_k V_{cR} (G_{km} \sin(\theta_k - \theta_{cR}) - B_{km} \cos(\theta_k - \theta_{cR})) + V_k V_{vR} (G_{vR} \sin(\theta_k - \theta_{vR}) - B_{vR} \cos(\theta_k - \theta_{vR})) \quad (13)$$

$$P_{mk} = V_m^2 G_{mm} + V_m V_k (G_{mk} \cos(\theta_m - \theta_k) + B_{mk} \sin(\theta_m - \theta_k)) + V_m V_{cR} (G_{mm} \cos(\theta_m - \theta_{cR}) + B_{mm} \sin(\theta_m - \theta_{cR})) \quad (14)$$

$$Q_{mk} = -V_m^2 B_{mm} + V_m V_k (G_{mk} \sin(\theta_m - \theta_k) - B_{mk} \cos(\theta_m - \theta_k)) + V_m V_{cR} (G_{mm} \sin(\theta_m - \theta_{cR}) - B_{mm} \cos(\theta_m - \theta_{cR})) \quad (15)$$

where G_{ij} , and B_{ij} ($i=k,m$ and $j=k,m$) are the elements making up the UPFC's general transfer admittance matrix, which is derived in the Appendix.

To guarantee that the UPFC neither absorbs nor injects active power with respect to the AC system, assuming a free loss converter operation, a mismatch equation $\Delta P_{DC-Link}^{upfc} = P_{bb} = P_{vR} + P_{cR} = 0$ must be considered. In this case, the active power supplied to the shunt converter, P_{vR} , must satisfy the active power demanded by the series converter, P_{cR} . These powers are given by,

$$P_{cR} = V_{cR}^2 G_{mm} + V_{cR} V_k (G_{km} \cos(\theta_{cR} - \theta_k) + B_{km} \sin(\theta_{cR} - \theta_k)) + V_{cR} V_m (G_{mm} \cos(\theta_{cR} - \theta_m) + B_{mm} \sin(\theta_{cR} - \theta_m)) \quad (16)$$

$$P_{vR} = -V_{vR}^2 G_{vR} + V_{vR} V_k (G_{vR} \cos(\theta_{vR} - \theta_k) + B_{vR} \sin(\theta_{vR} - \theta_k)) \quad (17)$$

4 FACTS STATE ESTIMATION ALGORITHM

In this section, the practical implementation of flexible AC transmission systems state estimation algorithm is described.

4.1 State Estimation FACTS Algorithm

The state estimation of power systems embedded with FACTS controllers can be assessed as described in section 2. In this case, the estimated state variables vector takes into account the nodal voltage magnitudes and angles, \hat{x}_{AC} , excluding the reference nodal angle, as well as the FACTS controllers state variables, \hat{x}_f ; i.e. $\hat{x} = [\hat{x}_{AC}, \hat{x}_f]$. Hence, the Jacobian matrix $H(\hat{x})$ is extended as follows,

$$H(\hat{x}_{AC}, \hat{x}_f) = \begin{bmatrix} \partial h_{AC}(\hat{x}_{AC}, \hat{x}_f) / \partial x_{AC} & \partial h_{AC}(\hat{x}_{AC}, \hat{x}_f) / \partial x_f \\ \partial h_{upfc}(\hat{x}_{AC}, \hat{x}_f) / \partial x_{AC} & \partial h_{upfc}(\hat{x}_{AC}, \hat{x}_f) / \partial x_f \end{bmatrix} \quad (18)$$

where $h_{AC}(\hat{x}_{AC}, \hat{x}_f) \in \mathbb{R}^m$ is the measurement vector and $h_{upfc}(\hat{x}_{AC}, \hat{x}_f) \in \mathbb{R}^{n_{UPFC}}$ is the measurement associated to the UPFC's DC-link mismatch equation $\Delta P_{DC-Link}^{upfc}$. Since the UPFC neither absorbs nor injects active power with respect to the AC system, the active power through the DC link is physically constrained to be zero. The constraint is treated as a zero power injection, such that no meter needs to be installed but the information is always available. This virtual measurement with relatively high weights is incorporated in the measurement set along with physically measured injections as shown in (18).

By way of example, it is assumed that a UPFC is connected between nodes k and m with measurements at

both terminals of branch powers, nodal voltage magnitudes and nodal power injections. The contribution of this controller to the whole power system Jacobian matrix (18) is given by (19). In this equation, the sign + indicates that the Jacobian element is linked to the nodal power injection measurement, and must be added with other Jacobian elements associated to the power flowing through transmission elements connected at the same node.

$$\begin{bmatrix}
 +\frac{\partial P_{km}}{\partial \theta_k} & +\frac{\partial P_{km}}{\partial \theta_m} & +V_k \frac{\partial P_{km}}{\partial V_k} & +V_m \frac{\partial P_{km}}{\partial V_m} & \frac{\partial P_{km}}{\partial \theta_{cR}} & V_{cR} \frac{\partial P_{km}}{\partial V_{cR}} & \frac{\partial P_{km}}{\partial \theta_{vR}} & V_{vR} \frac{\partial P_{km}}{\partial V_{vR}} \\
 +\frac{\partial P_{mk}}{\partial \theta_k} & +\frac{\partial P_{mk}}{\partial \theta_m} & +V_k \frac{\partial P_{mk}}{\partial V_k} & +V_m \frac{\partial P_{mk}}{\partial V_m} & \frac{\partial P_{mk}}{\partial \theta_{cR}} & V_{cR} \frac{\partial P_{mk}}{\partial V_{cR}} & 0 & 0 \\
 +\frac{\partial Q_{km}}{\partial \theta_k} & +\frac{\partial Q_{km}}{\partial \theta_m} & +V_k \frac{\partial Q_{km}}{\partial V_k} & +V_m \frac{\partial Q_{km}}{\partial V_m} & \frac{\partial Q_{km}}{\partial \theta_{cR}} & V_{cR} \frac{\partial Q_{km}}{\partial V_{cR}} & \frac{\partial Q_{km}}{\partial \theta_{vR}} & V_{vR} \frac{\partial Q_{km}}{\partial V_{vR}} \\
 +\frac{\partial Q_{mk}}{\partial \theta_k} & +\frac{\partial Q_{mk}}{\partial \theta_m} & +V_k \frac{\partial Q_{mk}}{\partial V_k} & +V_m \frac{\partial Q_{mk}}{\partial V_m} & \frac{\partial Q_{mk}}{\partial \theta_{cR}} & V_{cR} \frac{\partial Q_{mk}}{\partial V_{cR}} & 0 & 0 \\
 0 & 0 & V_k \frac{\partial V_k}{\partial V_k} & 0 & 0 & 0 & 0 & 0 \\
 0 & 0 & 0 & V_m \frac{\partial V_m}{\partial V_m} & 0 & 0 & 0 & 0 \\
 \frac{\partial P_{km}}{\partial \theta_k} & \frac{\partial P_{km}}{\partial \theta_m} & V_k \frac{\partial P_{km}}{\partial V_k} & V_m \frac{\partial P_{km}}{\partial V_m} & \frac{\partial P_{km}}{\partial \theta_{cR}} & V_{cR} \frac{\partial P_{km}}{\partial V_{cR}} & \frac{\partial P_{km}}{\partial \theta_{vR}} & V_{vR} \frac{\partial P_{km}}{\partial V_{vR}} \\
 \frac{\partial P_{mk}}{\partial \theta_k} & \frac{\partial P_{mk}}{\partial \theta_m} & V_k \frac{\partial P_{mk}}{\partial V_k} & V_m \frac{\partial P_{mk}}{\partial V_m} & \frac{\partial P_{mk}}{\partial \theta_{cR}} & V_{cR} \frac{\partial P_{mk}}{\partial V_{cR}} & 0 & 0 \\
 \frac{\partial Q_{km}}{\partial \theta_k} & \frac{\partial Q_{km}}{\partial \theta_m} & V_k \frac{\partial Q_{km}}{\partial V_k} & V_m \frac{\partial Q_{km}}{\partial V_m} & \frac{\partial Q_{km}}{\partial \theta_{cR}} & V_{cR} \frac{\partial Q_{km}}{\partial V_{cR}} & \frac{\partial Q_{km}}{\partial \theta_{vR}} & V_{vR} \frac{\partial Q_{km}}{\partial V_{vR}} \\
 \frac{\partial Q_{mk}}{\partial \theta_k} & \frac{\partial Q_{mk}}{\partial \theta_m} & V_k \frac{\partial Q_{mk}}{\partial V_k} & V_m \frac{\partial Q_{mk}}{\partial V_m} & \frac{\partial Q_{mk}}{\partial \theta_{cR}} & V_{cR} \frac{\partial Q_{mk}}{\partial V_{cR}} & 0 & 0 \\
 \frac{\partial P_{bb}}{\partial \theta_k} & \frac{\partial P_{bb}}{\partial \theta_m} & V_k \frac{\partial P_{bb}}{\partial V_k} & V_m \frac{\partial P_{bb}}{\partial V_m} & \frac{\partial P_{bb}}{\partial \theta_{cR}} & V_{cR} \frac{\partial P_{bb}}{\partial V_{cR}} & \frac{\partial P_{bb}}{\partial \theta_{vR}} & V_{vR} \frac{\partial P_{bb}}{\partial V_{vR}}
 \end{bmatrix} \quad (19)$$

In addition to the controller parameters estimation, it must be pointed out that this formulation is suitable to setting the FACTS controller parameters required to achieve both power and voltage control targets. In order to achieve this goal, the desired power flow and voltage magnitude are set as measurements.

4.2 State Variables Initial Conditions

In order to start the iterative process, it is necessary to provide initial conditions to the estimated state variables. These initial conditions are chosen based on engineering judgments. Nodal voltages are started from a flat profile; i.e. 1.0 pu for voltage magnitude and 0° for voltage angle. The initial condition for the TCSC's firing angle is chosen 8° away from the firing angle α_{RP} , which produce the TCSC's resonant point; i.e.

$\alpha_{TCSC}^0 = \alpha_{RP} + 8^\circ$. α_{RP} is calculated by (20). A similar approach is used to initialise the SVC's firing angle.

$$\alpha_{RP} = \pi \left(1 - \frac{\omega \sqrt{LC}}{2} \right) \quad (20)$$

For the UPFC, a set of equations which give good initial estimates can be obtained by assuming lossless UPFC and coupling transformers as well as null voltage angles in (12)-(15). By way of example, if branch power at UPFC's node m is measured, the initial conditions to the series voltage source are obtained by solving (14)-(15) which results in,

$$\theta_{cR}^0 = \arctan \left(\frac{P_{mk}^{measured}}{|C1|} \right) \quad (21)$$

$$V_{cR}^0 = \left(\frac{X_{cR}}{V_m^0} \right) \sqrt{(P_{mk}^{measured})^2 + C1^2} \quad (22)$$

where

$$C1 = Q_{mk}^{measured} - \frac{V_m^0}{X_{cR}} (V_m^0 - V_k^0) \quad (23)$$

An initialization for the shunt source angle can be obtained by substituting (16)-(17) into DC-link mismatch equation and solving for θ_{vR} . The resulting equation is,

$$\theta_{vR} = -\arcsin \left(\frac{(V_k^0 - V_m^0) V_{cR}^0 X_{vR} \sin(\theta_{cR}^0)}{V_{vR}^0 V_k^0 X_{cR}} \right) \quad (24)$$

Finally, if the shunt converter is acting as a voltage regulator, the voltage magnitude of the shunt source is initialised at the target voltage value. Otherwise, it is initialised at 1 pu.

4.3 Observability and Bad Data Analysis

For purposes of this paper, it is assumed that the network is observable. Bad data analysis is a post-estimation process that detects, identifies and eliminates the erroneous measurements. The detection is accomplished by the chi-square test [7, 9]. If bad data problem exist, the conventional largest normalised residual test is employed to identify single bad measurements [7]. The normalized residuals are obtained by the division of measurement residuals with their standard deviations,

$$\varepsilon_i^N = \frac{|\varepsilon_i|}{\sqrt{S_{ii}}}, \quad i = 1, \dots, m \quad (25)$$

where S_{ii} is the i -th diagonal element of the residual covariance matrix given by,

$$S = R - H[H^T R^{-1} H]^{-1} H^T \quad (26)$$

The normalized residuals are put in descending order of magnitude and the largest residual is removed first. A new WLS estimation is carried out with a reduced measurement vector and a bad data analysis is newly done. This process is repeated until bad data is not detected.

5 STUDY CASES

A WLS State Estimation program has been developed as discussed above to analyse FACTS. IEEE-30 node system embedded with 5 FACTS controllers, as shown in Figure 4, is used as a test system for all simulations. The IEEE-30 node system data can be found in [10]. The measurement set is assumed to be overdetermined, and it is generated by a power flow program. This set consists of 44 nodal power injections, 80 branch power flows and the UPFC's DC-link active power constraint. Two cases are simulated to show the effectiveness of the developed program [11].

5.1 State Estimation without measurements errors

This case considers no measurements errors. The state estimation results are validated with those given by a FACTS power flow program [2]. The TCSC reactance parameters are $X_C = 9.375e^{-3}$ pu and $X_L = 1.625e^{-3}$ pu. The initial condition of the firing angle is $\alpha_{TCSC}=145^\circ$. The SVC installed at node 19 is considered as a variable susceptance with an initial condition of $B=0.288$ pu. The SVC connected at node 30 is assumed without coupled transformer and reactances of $X_C = 1.07$ pu and $X_L = 0.288$ pu. The integrated SVC-transformer model is connected at node 15 with a transformer impedance of $Z_T=j 0.3$ pu and SVC's reactances of $X_C = 1.07$ pu and $X_L = 0.288$ pu. For the SVCs connected at nodes 15 and 30, the firing angle's initial condition is $\alpha_{SVC}=130^\circ$. Lastly, the UPFC coupling transformers have the same impedances $Z_{Vr} = Z_{Cr} = 0.05+j0.1$ pu.

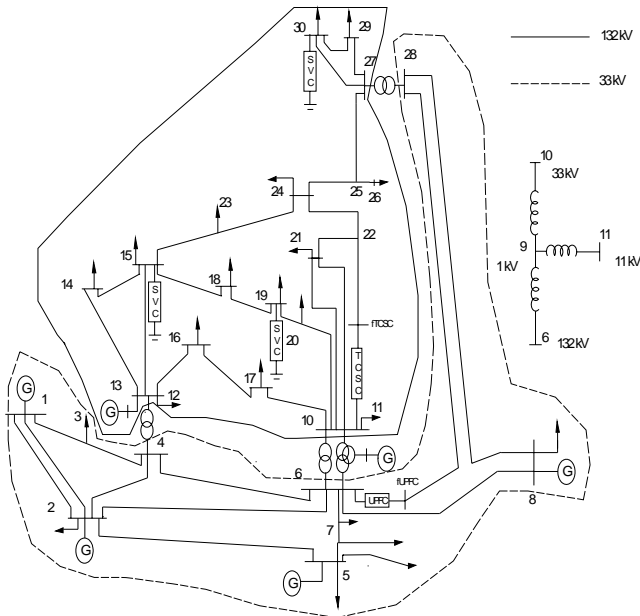


Figure 4: IEEE-30 node system with FACTS controllers.

The estimator is used to assess the required FACTS parameters in order to maintain the control targets given in Table 1.

FACTS Controller	Controlled Variable	Original Value	Target Value
SVC (B)	V_{19}	1.00284 pu	0.99 pu
UPFC	P_{6-28}	18.91 MW	10 Mw
	Q_{6-28}	1.4 MVar	4 Mvar
	V_6	1.00314 pu	1.05 pu
TCSC	P_{10-22}	7.404 MW	15 Mw
SVC (α)	V_{30}	0.97482 pu	1.0 pu
SVC-T	V_{15}	1.02256 pu	1.0 pu

Table 1: FACTS controllers control targets.

The state estimator converged in 7 iterations to a tolerance of $1e^{-4}$ with an optimally function's value

of $J(\hat{x})=9.848e^{-6}$. The estimated parameters of FACTS controllers as well as the UPFC converters powers are given in Tables 2 and 3, respectively. It must be observed that the UPFC's DC-link active power constraint has been fulfilled. These estimations were compared with the solution obtained by a FACTS power flow program [2]. The same results were arrived at.

FACTS Controller	FACTS Parameters	Estimated Values
SVC (B)	B_{SVC}	-0.0551464 pu
UPFC	$V_{CR} \angle \theta_{CR}$	0.018375 \angle 26.55
	$V_{VR} \angle \theta_{VR}$	1.21294 \angle -17.26
TCSC	α_{TCSC}	143.431 $^\circ$
SVC (α)	α_{SVC}	128.315 $^\circ$
SVC-T	α_{T-SVC}	122.236 $^\circ$

Table 2: Estimated FACTS parameters.

Source	Active Power	Reactive Power
Series	-0.0009	-0.0017
Shunt	-0.0009	2.0158

Table 3: UPFC converter powers.

5.2 State Estimation with measurements errors

The power system given in section 5.1 is analysed considering three bad data introduced in the measurements set as shown in Table 4. The bad data have been introduced at UPFC and TCSC locations where two measurements have been increased in value and one measurement has been changed in sign from negative to positive; i.e. the power flow has been diverted.

Measurement	Exact	Erroneous
Q_{10}	-0.02	-0.20
$P_{JUPFC-6}$	-0.1	-0.31
$Q_{JTCSC-10}$	-0.04629	0.04629

Table 4: UPFC converter powers.

The program correctly detects, identifies and eliminates the measurements errors as shown in Table 5. Once the bad data have been eliminated, the estimation converges in 6 iterations to a tolerance of $1e^{-4}$. The final estimation of FACTS parameters is equal to those given in Table 2.

Estimation	Erroneous Measurement	$J(\hat{x})$	$\chi_{k,\alpha}^2$	Iterations
1	$P_{JUPFC-6}$	641.78	80.266	8
2	Q_{10}	331.78	79.040	6
3	$Q_{JTCSC-10}$	80.349	77.812	6
4	None	1.09e-7	76.581	6

Table 5: State estimation with measurements errors.

6 CONCLUSIONS

A weighted least-square algorithm for the state estimation of power systems containing FACTS devices has been described in this paper. Guidelines and methods for implementing three FACTS controllers, namely TCSC, SVC and UPFC into the state estimator have been described in detail. Simulations are carried out on the IEEE-30 nodes system in order to illustrate the algorithm efficiency by numerical examples. The developed program is suitable to either estimate the FACTS controllers parameters under normal power system operation or to estimate these parameters values in order to achieve given control specifications, along with the power system state variables.

7 ACKNOWLEDGEMENTS

Authors gratefully acknowledge the financial support given to Mr. Zamora-Cardenas by the Consejo Nacional de Ciencia y Tecnología (CONACyT), México.

REFERENCES

- [1] N.G. Hingorani, "Flexible AC Transmission Systems", IEEE Spectrum, Vol. 30, No. 4, April 1993, pp. 40-15
- [2] E. Acha, C.R. Fuerte-Esquivel, H. Ambriz-Pérez and C. Angeles-Camacho, "FACTS: Modelling and Simulation in Power Networks", England, John Wiley & Sons, 2004, ISBN 0-470-85271-2, pp. 153-229
- [3] F.C. Schweppe and J. Wildes, "Power System Static-State Estimation-Part I:Exact Model", IEEE Trans. Power App. Syst., PAS-89, No. 1, pp. 120-125, January 1970
- [4] F.C. Schweppe and D.B. Rom, "Power System Static-State Estimation-Part II:Approximate Model", IEEE Trans. Power App. Syst., PAS-89, No. 1, pp. 126-130, January 1970
- [5] F.C. Schweppe, "Power System Static-State Estimation-Part III:Implementation", IEEE Trans. Power App. Syst., PAS-89, No. 1, pp. 130-135, January 1970
- [6] B. Xu and A.Abur, "State Estimation of Systems with UPFCs using the Interior Point Method", IEEE Trans. on Power Systems, Vol. 19, No. 3, pp 1635-1641, August 2004
- [7] A. Monticelli, "Electric Power system State Estimation", Proc. of the IEEE, Vol. 88, No. 2, pp 262-282, February 2000

- [8] L. Gyugyi, "A Unified Power Flow Control Concept for Flexible AC Transmission Systems", IEE Proceedings-C, Vol. 139, No. 4, pp 323-333, July 1992
- [9] A. Monticelli and A. García, "Reliable Bad Data Processing for Real-Time State Estimation", IEEE Trans. Power App. Syst., PAS-102, No. 3, pp 1126-1139, March 1983.
- [10] <http://www.ee.washington.edu/research/pstca/>
- [11] E.A. Zamora Cardenas, "State Estimation of Flexible AC Transmission Systems (In Spanish)", M.Sc. Thesis, Universidad Michoacana de San Nicolás de Hidalgo, September 2004.

APPENDIX

Derivations of UPFC equations are presented in this appendix. The general transfer admittance matrix for the UPFC is obtained by applying Kirchhoff current and voltage laws to the electric circuit shown in Figure 3, and it is given by equation (A.1).

$$\begin{bmatrix} \bar{I}_k \\ \bar{I}_m \end{bmatrix} = \begin{bmatrix} \bar{Y}_{kk} & \bar{Y}_{km} & \bar{Y}_{km} & \bar{Y}_{vR} \\ \bar{Y}_{mk} & \bar{Y}_{mm} & \bar{Y}_{mm} & 0 \end{bmatrix} \begin{bmatrix} \bar{V}_k \\ \bar{V}_m \\ \bar{V}_{cR} \\ \bar{V}_{vR} \end{bmatrix} \quad (\text{A.1})$$

where

$$\bar{y}_{cR} = \frac{1}{\bar{z}_{cR}} = \frac{1}{R_{cR} + jX_{cR}} \quad (\text{A.2})$$

$$\bar{y}_{vR} = \frac{1}{\bar{z}_{vR}} = \frac{1}{R_{vR} + jX_{vR}} \quad (\text{A.3})$$

$$\bar{Y}_{kk} = G_{kk} + jB_{kk} = \bar{y}_{cR} + \bar{y}_{vR} \quad (\text{A.4})$$

$$\bar{Y}_{mm} = G_{mm} + jB_{mm} = \bar{y}_{cR} \quad (\text{A.5})$$

$$\bar{Y}_{km} = \bar{Y}_{mk} = G_{km} + jB_{km} = -\bar{y}_{cR} \quad (\text{A.6})$$

$$\bar{Y}_{vR} = G_{vR} + jB_{vR} = -\bar{y}_{vR} \quad (\text{A.7})$$

Based on the equivalent circuit shown in Figure 3 and equation (A.1), the active and reactive power equations injected at UPFC terminals k and m are given by (A.8) and (A.9), respectively. From these equations, (12)-(15) are obtained.

$$P_{km} = \Re_e \{ \bar{V}_k \bar{I}_k^* \} \quad Q_{km} = \Im_m \{ \bar{V}_k \bar{I}_k^* \} \quad (\text{A.8})$$

$$P_{mk} = \Re_e \{ \bar{V}_m \bar{I}_m^* \} \quad Q_{mk} = \Im_m \{ \bar{V}_m \bar{I}_m^* \} \quad (\text{A.9})$$